African Journal of Biological Sciences

Journal homepage: http://www.afjbs.com

Research Paper   **Open Access**

Comparison of Non-Decellularized, Decellularized Freeze-Dried Bovine Bone, and Deproteinized Bovine Bone Material Morphology

Astrid Bernadette Ulina Purba[1], Ni Putu Mira Sumarta[2], RM Coen Pramono Danudiningrat[3], Andra Rizqiawan[4], M Subhan Amir[5], Devi Rianti[6], David Buntoro Kamadjaja[7]

[1]Resident, Department of Oral and Maxillofacial Surgery, Faculty of Dental Medicine, Universitas Airlangga /Universitas Airlangga Dental Hospital, Surabaya, Indonesia
[2,3,4,5,7]Staff, Department of Oral and Maxillofacial Surgery, Faculty of Dental Medicine, Universitas Airlangga / Universitas Airlangga Dental Hospital, Surabaya, Indonesia
[6]Staff, Dental Material Department, Faculty of Dental Medicine, Universitas Airlangga, Surabaya, Indonesia
Emails: [7]david-b-k@fkg.unair.ac.id

ABSTRACT

Background: Cancellous bovine bone scaffold, as a temporary 3-D framework, initiates human extracellular matrix morphology with a porosity of 50-90%, pore size of 100-1000 μm, and is heterogeneous and anisotropic. Researchers have developed various conventional techniques to form better morphology. The Cell and Tissue Bank of RSUD Dr. Soetomo developed Deproteinized Bovine Bone Material (DBBM) from local bovine bone by thermal deproteinization, heated to 1000°C, leaving only inorganic components that are hard to degrade. Freeze-Dried Bovine Bone (FDBB) is produced through lyophilization, retaining organic components that are potentially immunogenic, thus requiring further decellularization (DC-FDBB) using Sodium Dodecyl Sulphate (SDS) to remove these components and increase porosity, while still maintaining extracellular matrix structure. Previous studies have not presented complete data on the morphology of these materials.
Aim: The study aims to compare the morphology of FDBB, DC-FDBB, and DBBM scaffolds.
Material and Methods: Five cube-shaped of FDBB, DC-FDBB, and DBBM group were observed for porosity, pore size, trabecular thickness, number of trabeculae, degree of anisotropy, connectivity density, bone surface density, and structure model index using Micro CT. Comparative analysis using ANOVA test was subsequently carried out to evaluate the differences in these variables among the groups.
Results: FDBB and DBBM differed significantly in porosity (p = 0.002), pore size (p = 0.004), degree of anisotropy (p = 0.008), and structure model index (p = 0.008) with Post Hoc Tukey HSD. FDBB and DC-FDBB significantly differed in porosity only (p = 0.031). DC-FDBB and DBBM significantly differed in connectivity density (p = 0.020) and structure model index (p = 0.002).
Conclusion: The most ideal microarchitecture morphology were DBBM and the least were DC-FDBB.

Keywords: The most ideal microarchitecture morphology were DBBM and the least were DC-FDBB.

1. Introduction

Extensive bone defects due to trauma, tumors, and congenital diseases provide challenges for maxillofacial surgeons in performing reconstruction need tissue engineering (Nelms & Palmer, 2019). Researchers developed scaffolds with different biomaterials such as bovine with similar structure to extracellular bone matrix and different conventional techniques to form better architectural morphology 3D scaffold through heating, freeze drying, and decellularization (Bagwan et al., 2021). The 3D scaffold matrix provides a physical environment that guides cell colonization in all directions, offering a spatiotemporal configuration similar to in vivo conditions. This environment can affect cell morphology, alignment, orientation, multicellular organization, cell spreading, and attachment (Cheung et al., 2007; Lawrence & Madihally, 2008); with minimum pore size 100μm, 200-500μm for capillary formation, and 100-1000μm for bone growth (Sari et al., 2021); porosity of 55-70% for growth into blood vessels, porous with interconnected network to allow diffusion of nutrient, exchange of oxygen, and disposal metabolic wastes; provide sufficient mechanical strength, biocompatible, bioresorbable, and biodegradable scaffold (Lawrence & Madihally, 2008).

An ideal bovine cancellous bone scaffold should have a morphology similar to human cancellous bone with porosity of 50-90%, highly heterogeneous, and anisotropic (Oftadeh et al., 2015). The microarchitecture morphology cancellous bovine bone is very complex, including porosity of 45,5-72,70%, pore size of 0,458mm±0,115mm, trabecular thickness of 0,243±0,027mm, anisotropy degree of 0,599±0,139, connectivity density of 4,588±2,053, and structural model index of 0,631±0,652 (Ashworth et al., 2014; Fatihhi et al., 2015). Higher porosity and pore interconnectivity could lead to increases the overall surface area for cell attachment and facilitates cell ingrowth in the scaffolds. Pore size of microporous scaffolds increases the number of pore within scaffold. Trabecular matrix thickness, orientation, and shape must be evaluated mimic in vivo condition and produce more matrix extracellular (Lawrence & Madihally, 2008).

Cell and tissue bank of RSUD Dr. Soetomo developed Deproteinized Bovine Bone Material (DBBM) from local bovine bone by thermal deproteinization heated to 1000°C, has a pore size of 200-500μm with 35x SEM magnification, leaving only inorganic components, with good pore interconnectivity, affordable processing fee and a good quality resembling foreign made materials (Ferdiansyah Mahyudin & Utomo, 2018; Kamadjaja et al., 2017). It has a chemical composition and architectural geometry that is almost identical to human bone (osteoconductive), more acceptable to the host body because it reduces antigenic factors, but difficult to degrade, causing development of FDBB (Kartikasari et al., 2016; Lei et al., 2015).

Freeze Dried Bovine Bone (FDBB) has gone through frozen and dried or lyophilized to maintain the physical and chemical structure also suppressing excessive antigen reactions that can occur. It contains organic and inorganic components therefore it could be completely absorbed by the body, and it is able to support bone regeneration (Humidat et al., 2018). It needed free antigenic potential thus requiring further decellularization (DC-FDBB) using Sodium Dodecyl Sulphate (SDS) which is expected to remove residual cells, DNA, alpha gal epitope, increase porosity bovine cartilage, but still maintain extracellular matrix structure with a wide area and sufficient space between the bone structure thus maximizing decellularization process (Cravedi et al., 2017; Gardin et al., 2015). DBBM, FDBB and DC-FDBB cancellous bovine bone scaffold were used in this study are development materials in Surabaya that never been subjected to complete morphological test.

Morphological analysis of cancellous bovine bone scaffold with micro-CT is the gold standard, providing quantitative and qualitative analysis informations, as well as visualization of geometry by converting 2D cross sectional files into intact 3D (Bigham-Sadegh & Oryan, 2015). Previous studies have not presented complete data on morphology of FDBB, DC-

FDBB, and DBBM, thus the researcher conducted this research.

2. Methodology

This observational laboratory study was to compare the morphology of bovine-derived scaffolds processed in different ways i.e. freeze-drying (FDBB), decellularization (DC-FDBB), and deproteinization (DBBM). This research has received ethical approval issued by the ethics committee of the Faculty of Dental Medicine, Universitas Airlangga numbered 455/HRECC.FODM/VII/2022.
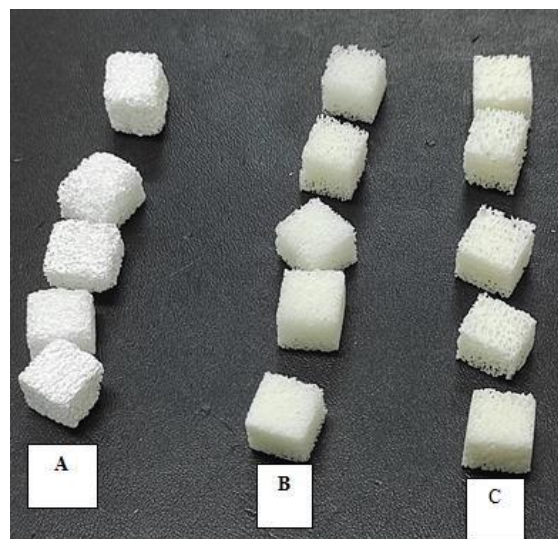
Scaffolds Preparation

Figure 1. Cancelous bovine bone scaffolds 10x10x10mm: DBBM scaffold (a), FDBB scaffold (b), and DC-FDBB scaffold (c)

The samples were processed in the Cell and Tissue Bank, Dr. Soetomo Surabaya from cancellous bovine femur bone in the form of cubes of 10x10x10mm (Figure 1). These scaffolds were manufactured according to the following protocol:

The first step of FDBB scaffold production began with taking several pieces of cancellous bone in the bovine femur region in the form of blocks with the maximum size that could be obtained. The bones were soaked in a 3% hydrogen peroxide solution to remove any residual blood, fat, and bone marrow rinsed with sterile distilled water to clean the remaining peroxide solution. After washing, the bovine bones were dried by freeze-drying method at -80°C and dried with a lyophilizer until the moisture content was below 10%.

The decellularization method FDBB (DC-FDBB) was with Sodium Dodecyl Sulfate (SDS). The samples were stored at 4°C and then rinsed with phosphate buffer saline (PBS) solution before SDS was administered with a concentration of 0.5% for 1 hour. Samples were rinsed with sterile distilled water and PBS, scaffolds were placed on a stirrer and rinsed with a solution containing chloroform and ethanol, with an initial ratio of 2:1 for 24 hours. Followed by freeze drying, which is cooling at -80°C and dried with lyophilizer until the water content was below 10%.

The DBBM manufacturing process began by taking pieces of cancellous bone in the bovine region in the form of blocks with the maximum size that can be obtained. The bones were washed with hydrogen peroxide and 0.9% NaCl to remove the remnants of fat. The deproteination process was carried out by burning samples at temperature of 1000°C, rinsed with sterile distilled water. The scaffold was dried in the oven at a temperature of 100°C. The

next step was packing or wrapping the scaffold in two layers, tightly sealed and sent for sterilization using gamma ray radiation.

Scaffold Examination

The sample examination was carried out at the Medical Devices and Technology Center (MEDITEC) Institute of Human Center and Engineering (iHumEn) University Technology Malaysia (UTM), Skudai, Johor, Malaysia with Micro CT 1272 Skyscan. Scaffold was scanned dry with image pixel size (spatial resolution) 17,2μm, voltage source 100kV, current source 100μA, Al filter 0,5mm, autonomic segmentation is performed to distinguish which part is pore (black) and which part is trabecular (white), also known as binary thresholding, in principle determine the dividing limit on the image data set with a grayscale value between 0-255 (8-bit image). Scan time was approximately 4 hours for each sample with 980 scan slices, 3D sample built with Finite element simulation, using 3 scans, the upper scan was taken at 40th slice, the middle scan was taken at 400th slice, and the lower scan was taken at 800th slice. The morphology of scaffold revealed that the lighter color projected a larger pore size (black = 0; white 808,81-843,23μm) and thicker pore (black = 0; white = 430,22- 464,64μm).

Analysis of scaffold structure includes pore size, trabecular spacing, trabecular thickness, trabecular number in all specimens was performed in 3D using a sphere-fitting algorithm, and analysis of porosity, degree of anisotropy, connectivity density, bone surface density, structure model index was performed using CT-An (Bruker) software. Data collection were carried out at the Laboratory of Rock Physics FMIPA Institute Technology Bandung, while data processing and compilation of results performed Faculty of Dental Medicine, Universitas Airlangga Surabaya, Indonesia.

Statistical Analysis

Statistical analysis was performed using IBM SPSS version 25. Shapiro-wilk distribution normality test, Levene's homogeneity test, one-way ANOVA followed by Post Hoc Tukey HSD were carried out to determine the differences among groups.

3. Results and Discussion

Results

The result 3D morphology of FDBB scaffold revealed that trabecular thickness of FDBB is sufficiently high, the pore size slightly large, and is interconnected with each other on all sides. The trabecular thickness of the lower scan FDBB scaffold was larger than the upper and middle scan, marked by yellow and white color domination, on the other hand the pore size shrunk (Figure 2). Trabecular thickness of DC-FDBB was relatively low, with large pore size, and was interconnected with each other on all sides. The trabecular thickness of the upper, middle, and lower scan DC-FDBB scaffold was thinner, marked by blue and purple color domination, heterogenous in form, trabecular arrangement is irregular and damaged, on the other hand towards the lower scan, the pore size was enlarged (Figure 3).
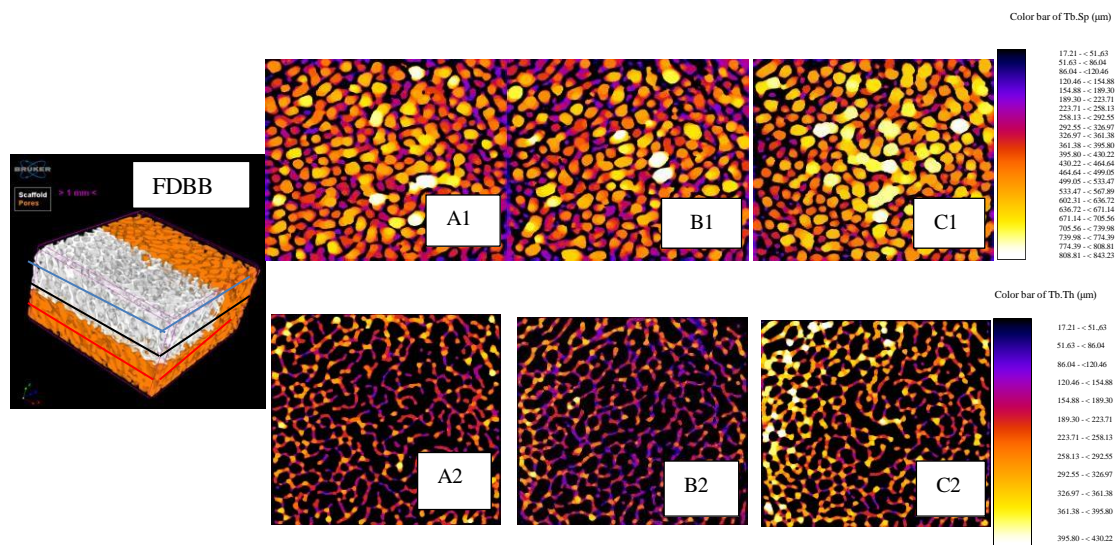
Figure 2. FDBB 3D scaffold morphology with micro CT ; Pore size upper scan (A1); middle scan (B1); lower scan (C1); trabecular thickness upper scan (A2); middle scan (B2); lower scan (C2)

Figure 3. DC-FDBB 3D scaffold morphology with micro CT; Pore size upper scan (A1); middle scan (B1); lower scan (C1); trabecular thickness upper scan (A2); middle scan (B2); lower scan (C2)
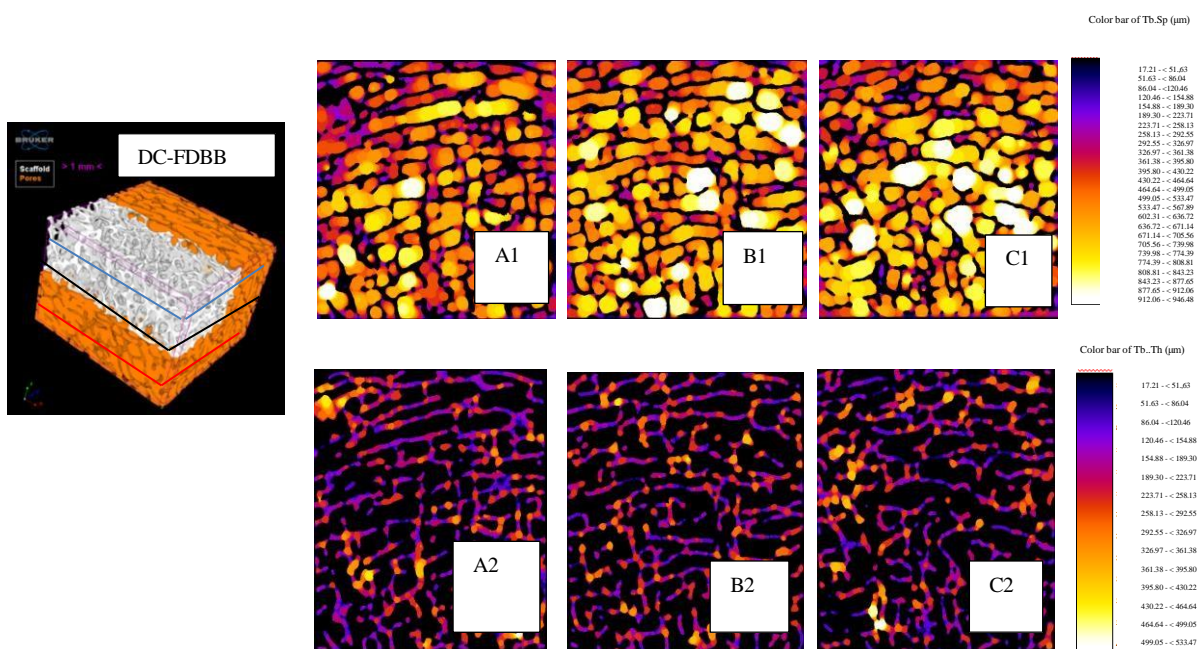
The trabecular thickness of DBBM was relatively low, had larger pore size, and was interconnected with each other on all sides. The pore size of the upper, middle, and lower scan DBBM scaffold was larger in size, marked by yellow and orange domination, heterogenous in form, trabecular arrangement was regular relatively and trabecular thickness was relatively thin but not damaged (Figure 4).
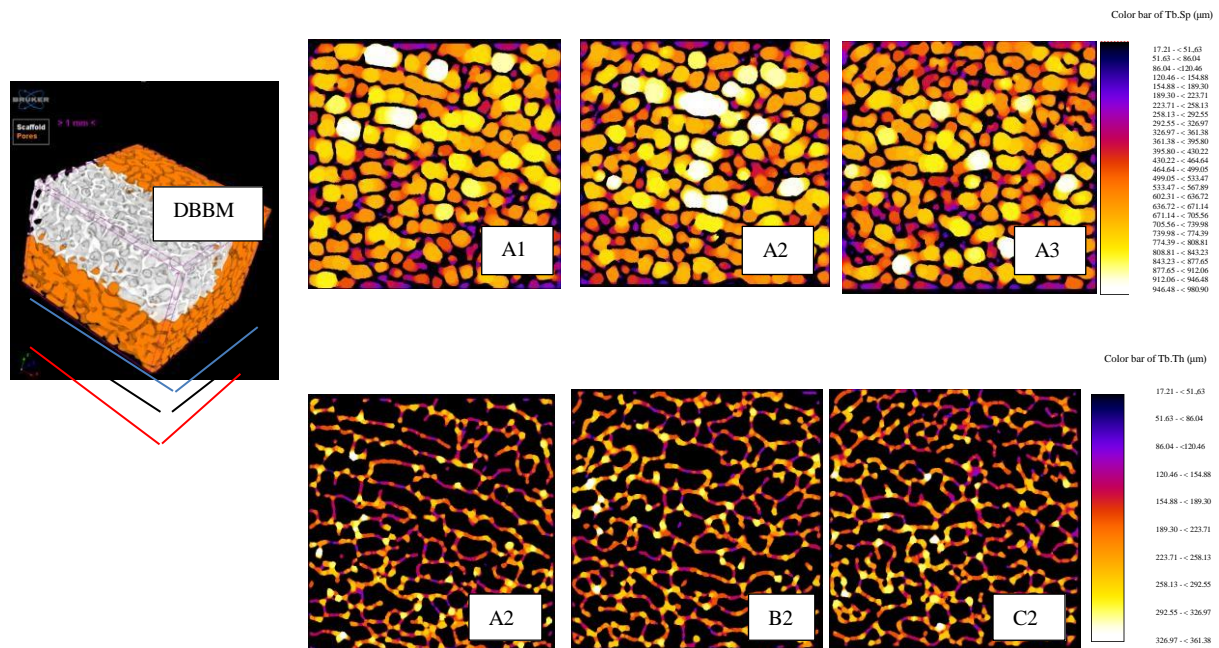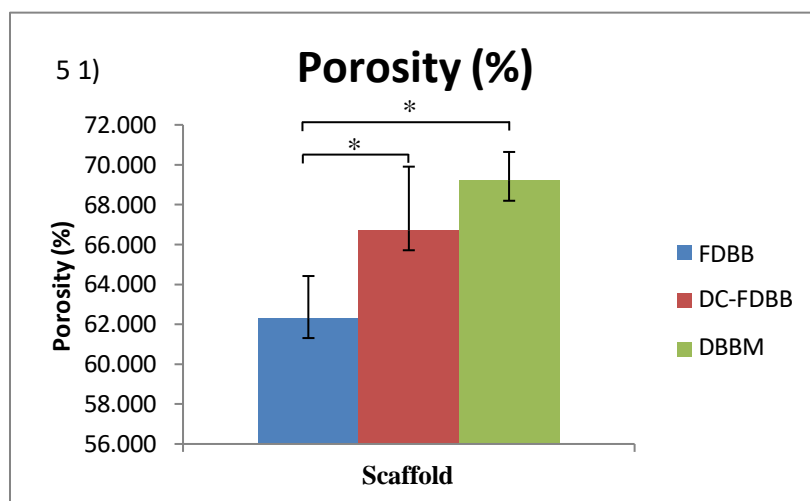
Figure 4. DBBM 3D scaffold morphology with micro-CT; Pore size upper scan (A1); middle

The results of calculation mean, standard deviation and Post hoc Tukey of morphology component (porosity, pore size, degree of anisotropy, structure model index, connectivity density) FDBB, DC-FDBB, and DBBM can be seen in figure 5 and table 1.

5.2)

Pore Size (µm)

5 3)

Trabecular Thickness (µm)

5. 4)

Trabecular Number (mm-1)

5. 5)

Degree of Anisotropy

5.6

Connectivity Density (mm^{-3})

5.7

Bone Surface Density (mm²/mm³)

5.8)
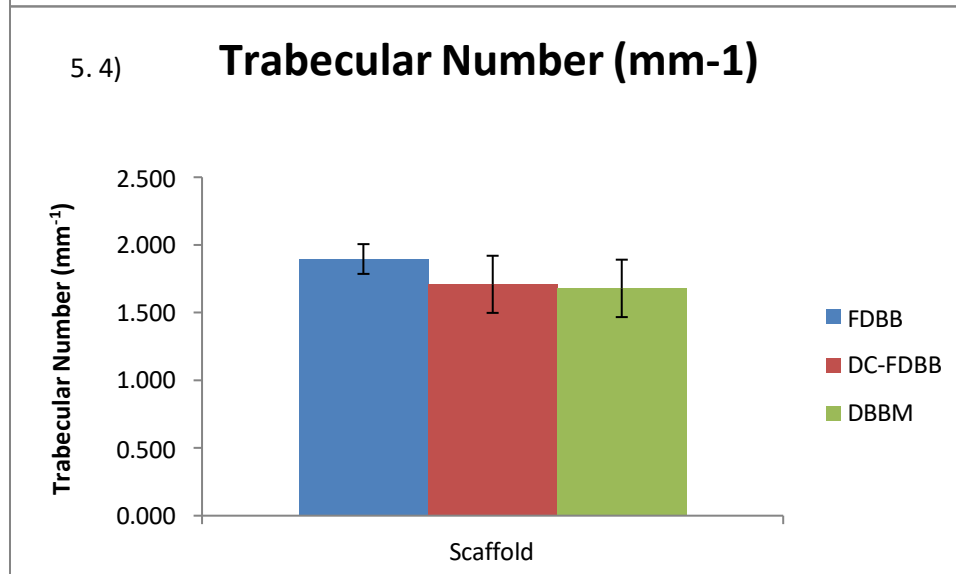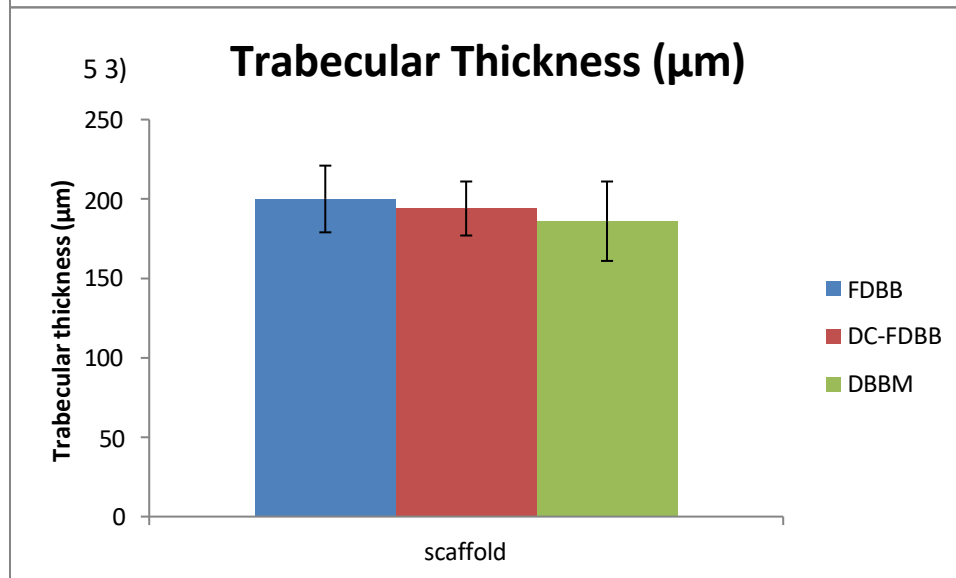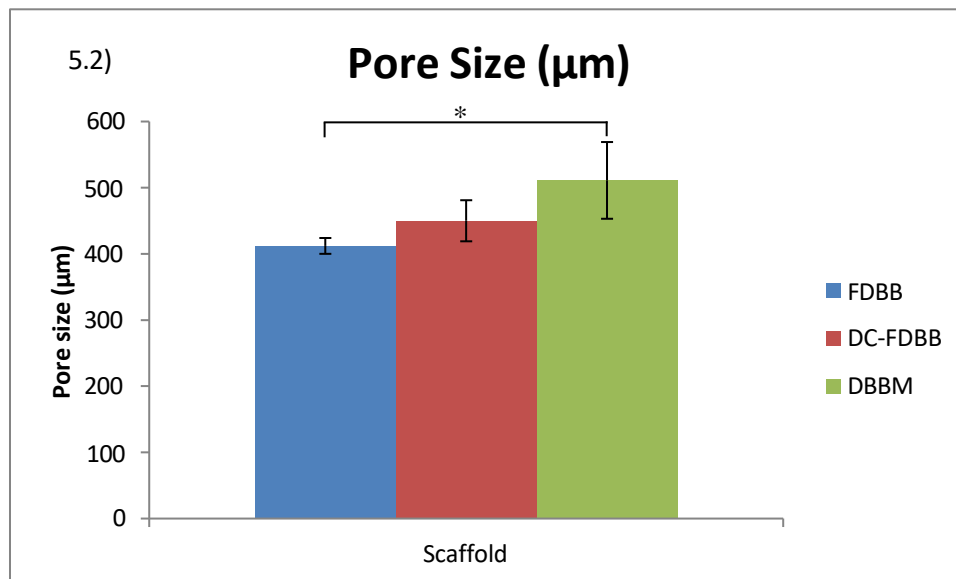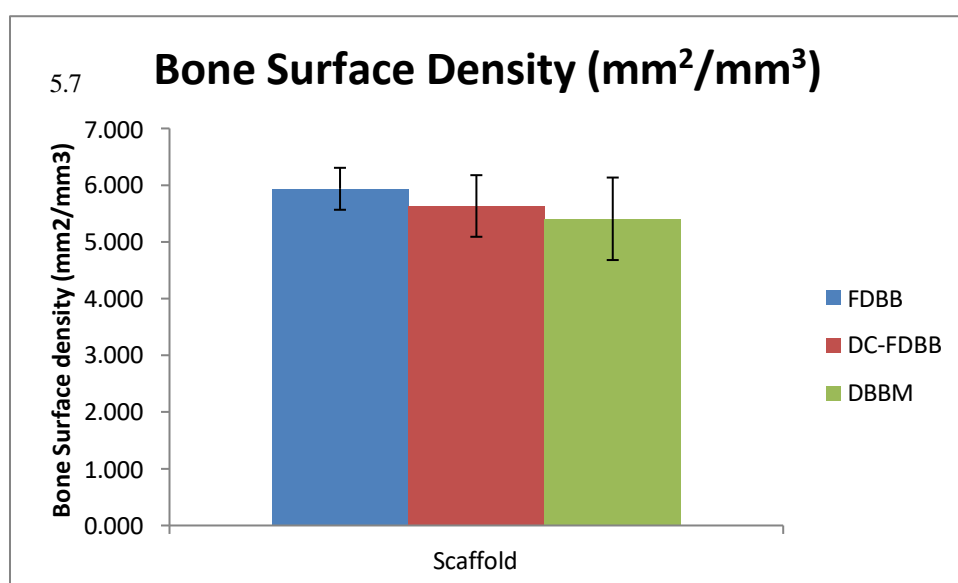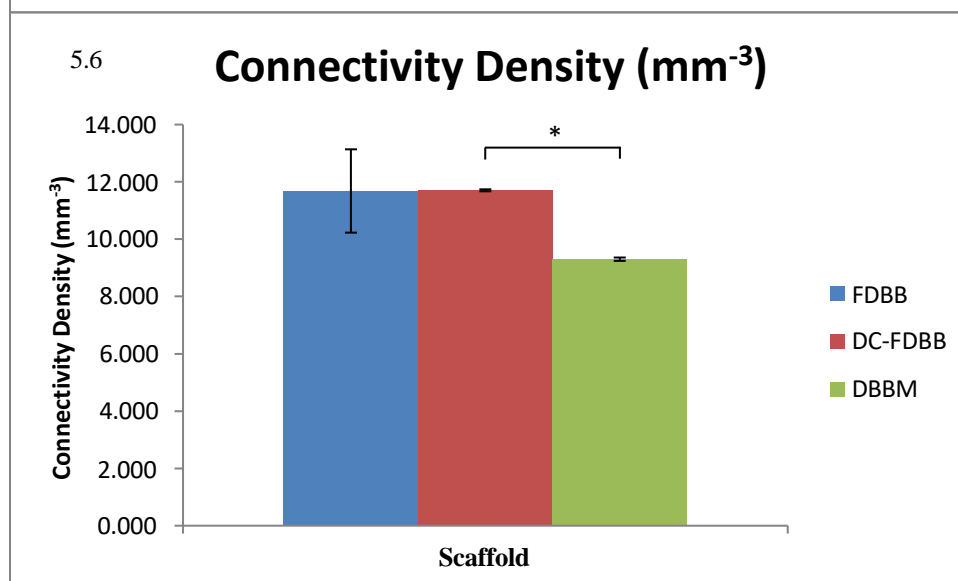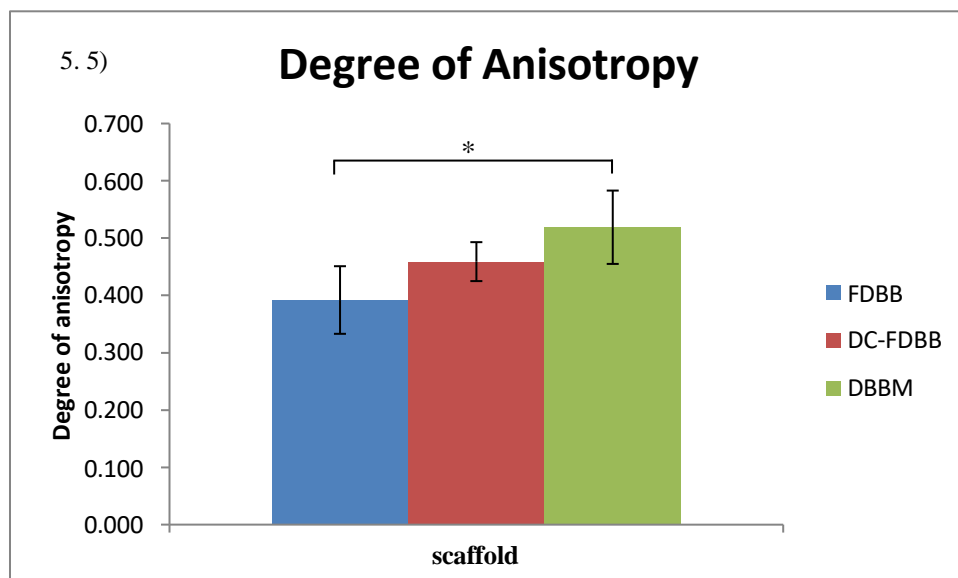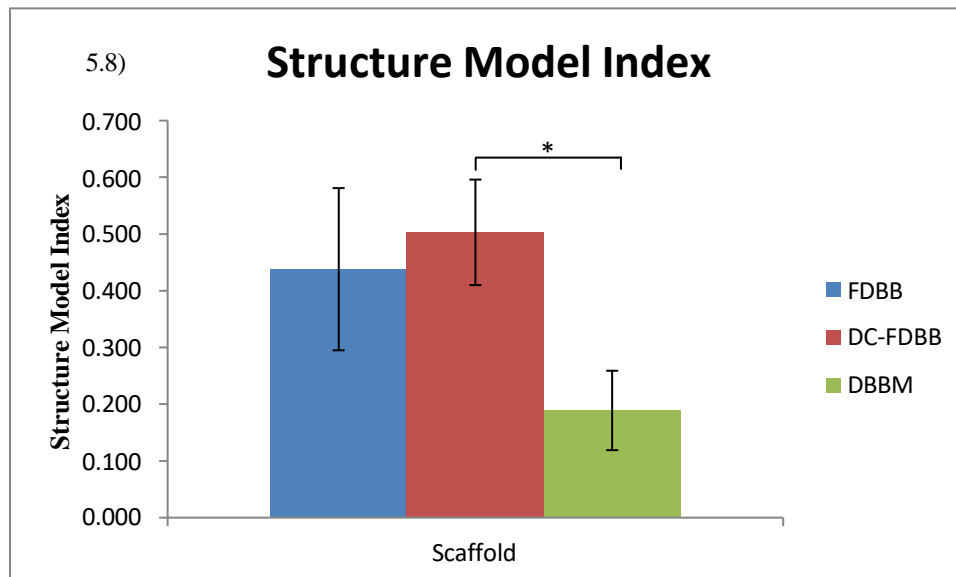
* Post Hoc *p-value* <0.05 significant different

Figure 5. Mean, standard deviation, and Post Hoc Tukey HSD Morphology Component: 5.1 Porosity graphics; 5.2 Pore size graphics; 5.3 Trabecular thickeness graphics; 5.4 Trabecular number graphics; 5.5 degree of anisotrophy graphics; 5.6 Connectivity density graphics; 5.7 bone surface density graphics; 5.8 Structure model index graphics;

Table 1. Calculation Result of Morphology Component and statistical analysis of Scaffold FDBB,DCFDBB, and DBBM

Morphology Component	N	Scaffold type	Mean	Standart deviation	Saphiro-Wilk test	Levene test	One Way ANOVA test	Standard
Porosity	5	FDBB	62,310 %	2,111%	0,522*	0,307*	0,002**	50-90% (Ashworth et al., 2014) 45,5-72,70% (Ferdiansyah Mahyudin & Utomo, 2018)
	5	DC-FDBB	66,712 %	3,192%	0,980*			
	5	DBBM	69,194 %	1,447%	0,367*			
Pore size (Tb.Sp)	5	FDBB	412 μm	12 μm	0,992*	0,109*	0,006**	91,2-497,8μm (Fernandez de Grado et al., 2018) 200-500 μm (Bouxsein et al., 2010) 300-500 μm (Migliaresi & Motta, 2014)
	5	DC-FDBB	450 μm	31μm	0,492*			100-1000μm (Krieghoff et al., 2019)

	5							200-500 μm (Bouxsein et al., 2010) 300-500 μm (Migliaresi & Motta, 2014)
	5	DBBM	511μm	58μm	0,843*			200-500 μm (Kamadjaja et al., 2017) 300-500 μm (Migliaresi & Motta, 2014)
Trabecular Thickness (Tb.Th)	5	FDBB	200μm	21 μm	0,996*	0,529*	0,613	243±27 μm (Ferdiansyah Mahyudin & Utomo, 2018)
	5	DC-FDBB	194μm	17 μm	0,918*			
	5	DBBM	186 μm	25 μm	0,308*			
Trabecular number (Tb.N)	5	FDBB	1,896	0,110	0,600*	0,539*	0,173	1,66±0,13 mm^{-1} (Cahyaningrum et al., 2018)
	5	DC-FDBB	1,709	0,211	0,172*			
	5	DBBM	1,679	0,212	0,732*			
Degree of anisotropy	5	FDBB	0,392	0,059	0,378*	0,230*	0,010**	0,599±0,139 (Ferdiansyah Mahyudin & Utomo, 2018)
	5	DC-FDBB	0,459	0,034	0,685*			
	5	DBBM	0,519	0,064	0,097*			
Connectivity Density (Conn.D)	5	FDBB	11,682	1,454	0,922*	0,524*	0,018**	4,588±2,053 mm^{-3} (Ferdiansyah Mahyudin & Utomo, 2018)
	5	DC-FDBB	11,076	0,034	0,296*			
	5	DBBM	9,301	0,059	0,212*			
Bone Surface Density (BSD)	5	FDBB	5,936	0,370	0,948*	0,071*	0,356	0,201±0,022 mm^2/ mm^3 (Ferdiansyah Mahyudin & Utomo, 2018)
	5	DC-FDBB	5,633	0,543	0,144*			
	5	DBBM	5,407	0,727	0,216*			
Structure Model Index (SMI)	5	FDBB	0,438	0,143	0,715*	0,239*	0,001**	0,631±0,652 (Ferdiansyah Mahyudin & Utomo, 2018) SMI =3 perfect rods SMI=0 perfect plates (Murphy et al., 2013)
	5	DC-FDBB	0,503	0,093	0,546*			
	5	DBBM	0,189	0,070	0,907*			

* *p-value* >0.05 normally distribution/homogen

**p-value <0.05 significant different

Discussions

Cancellous bovine bone scaffolds which were depicted on micro CT showed a honey comb-like structure, heterogenous shape such as round, ellipsoidal, highly anisotropic, consisting of interconnected trabeculae (Mitchell & Tojeira, 2013). Conventional fabrication methods such as freeze drying and heating affect porosity, pore size, shape surrounding

tissue, do not have sufficient control, thus causing suboptimal 3D scaffold because creating uniform pore size and distribution with porous 3D matrix is a common problem (Bahraminasab, 2020; Lawrence & Madihally, 2008).

Porosity is the percentage of pores in a volume of material. In this study, the average porosity of DBBM showed the greatest results, significantly different from porosity of FDBB, This is accordance with the theory that fabrication of DBBM requires heating up to 1000°C to dissolve all organic components, leaving only inorganic components, decomposition of carbonate minerals and transformation of hydroxyapatite into three calcium phosphate (β-TCP), this makes the porosity larger thus increases osteogenesis but decrease mechanical strength, large connectivity structure, conversely trabecular thickness decreases in size, and Ca/P ratio is reduced thus resorption becomes slower and solubility decreases (Abdelmoneim et al., 2020; Niakan et al., 2015; Uklejewski et al., 2015).

FDBB porosity significantly differs from DC-FDBB, and this is accordance with the theory of FDBB process making which only requires 2 processes, namely freezing in -80°C which forms ice crystals, followed by drying with vacuum freeze dry until ice crystals sublimate to form pores until the water content is <8%, which makes porosity greater, while the mineral composition of microstructure and protein content remains unchanged. While on DC-FDBB it begins with decellularization first using 0,5% SDS for 24 hours then freezing and drying, which dissolves cytoplasm, damage cell membrane proteins, removes glycosaminoglycans causing water loss, breakdown matrix structure, resulting in higher connectivity and anisotropy degree (Gardin et al., 2015). Shahabipour et al (2013) stated that immersion with 2,5% SDS for 8 hours was effective to eliminate cells in cancellous bovine bone but did not damage the extracellular matrix.

This study showed that the largest pore size in DBBM that showed significant difference with FDBB scaffold, this is in accordance with the statement of Ferdiansyah Mahyudin & Utomo (2018), that heating/annealing to 1000°C increases pore size because of deproteinization and decarbonization, leaving only inorganic components with pore sizes of 200-500μm, while the pore size of FDBB according to Galia et al (2011) in the range of 91,2-497,8μm because ice crystals sublimate to form pores until the water content is <8%, which makes pore, it still contains protein and mineral composition.

These three types scaffold are still in range of scaffold pore sizes from bovine cancellous bovine bone according to Fatihhi et al (2015) which is between 458 ± 115 μm; still considered an ideal pore size for tissue engineering for bone growth that requires a pore size of 100-1000μm (Sari et al., 2021); pore size 300-500 μm provide the best results or collagen production, hydroxyapatite deposition, and bone mineral maturation (Krieghoff et al., 2019). Bone regeneration requires a pore size of 100-350μm and fibrovascular tissue requires a pore size of 500 μm (Migliaresi & Motta, 2014). Pore size 200-350μm optimal for osteoblast proliferation and is osteoconductive (Oryan et al., 2014). This is in accordance with the pore size should not be too small or too large, if too small than 100μm can inhibit migration, penetration, can form cellular capsule at the edge of the scaffold which limits the diffusion of nutrients and the disposal of metabolic wastes resulting necrosis of the core of the scaffold (Murphy et al., 2013).

The thickness of trabecular bone plays a crucial role in the bone healing process, particularly in trabecular bone fractures. The healing of trabecular bone involves intramembranous ossification, where a small callus is initially formed, followed by the development of woven bone, and eventually remodeling into regular trabecular bone (Soleimanifar & Katoozian, 2013). In metaphyseal fractures, cancellous bone primarily heals through the formation of intertrabecular bone, which is spatially limited and specific to cancellous bone, with minimal involvement of cartilage (Sandberg & Aspenberg, 2016). Trabecular metals, biomaterials used in reconstructive surgery, enhance biological growth and provide structural support in cases of severe bone deficits, highlighting the importance of

trabecular architecture in bone healing and recovery (Stiehl, 2005).

Trabecular thickness is organized to optimize load transfer, with increased porosity resulting in greater surface area but reduced strength. Additionally, resorption takes place along the bone surface. Thinner trabeculae are resorbed first, thereby increasing the mean thickness that trabeculae remain adapt to increasing mechanical demand with regard to fracture risk prediction. In this study, the largest trabecular thickness is in the FDBB group, because FDBB had the smallest porosity and pore size, and in the morphology description FDBB was dominated by yellow and white colors, while DC-FDBB was dominated by purple and blue colors which represents thin trabeculae. DBBM is dominated by orange color which indicates that it is thicker than DC-FDBB but thinner than FDBB. In SPSS it was concluded that trabecular thickness in these three scaffolds did not have a significant difference because in DC-FDBB with decellularization using SDS 0,5% for 24 hours extracellular matrix damage was observed (Abdelmoneim et al., 2020; Niakan et al., 2015; Uklejewski et al., 2015).

The number of trabeculae in bone healing are required because bone remodelling only occurs on the internal surface of bone matrix, matrix disruption maybe expected to disrupting their attachment to bone matrix, interrupting their communication and metabolic exchange. Trabeculae play a crucial role in bone healing by providing a scaffold for bone formation and inward growth, influencing mechanical strength, and enhancing osteogenic ability. Research has indicated that scaffolds such as trabecular structures exhibit superior osteogenic potential due to their irregular structure, which creates a diverse mechanical stimulation environment that aligns with the demands of bone regeneration (Liang et al., 2022). The results showed that the mean number of trabeculae was the largest in the FDBB group and the smallest in the DBBM group. However, the SPSS analysis concluded that there was no significant difference in the number of trabeculae among FDBB, DC-FDBB, and DBBM. This can occur because the basic material of cancellous bovine bone has very heterogeneous and anisotropic morphologies, and the conventional method did not provide sufficient control, thus causing suboptimal 3D scaffolds (Bahraminasab, 2020). According to Morgan et al (2004), bovine bone has a number trabecula $1,66 \pm 0,13$ mm^{-1} so these three scaffold still in standard number of trabeculae as scaffolds.

The degree of anisotropy creates an optimized three dimensional microarchitecture to meet the functional demands of bone and support mechanical loading. Structural anisotropy has a direct influence on stiffness properties as well as strength, directly synthesise new bone matrix on the bone surface. Degree of anisotropy is measure of how highly substructures are within a volume. Research has shown that bones are inherently anisotropic due to the composition of collagen and hydroxyapatite, which results in differences in electric potential induced by ultrasound irradiation based on the direction of wave propagation (Matsukawa et al., 2017). Anisotropic scaffolds, mimicking cortical bone, have been found to enhance osteoconductive properties and improve bone regeneration ability by increasing the efficiency of bone morphogenetic protein such as rhBMP-2, ultimately enhancing bone healing (Stuckensen et al., 2019). Anisotropic scaffolds with axially aligned channels have demonstrated accelerated bone growth compared to isotropic scaffolds, indicating their potential in bone tissue engineering applications (Li et al., 2016). In this study, the highest degree of anisotropy was DBBM and the smallest FDBB. There was only a significant difference in the degree of anisotropy of DBBM and FDBB, while the degree of anisotropy of scaffolds FDBB and DC-FDBB and DC-FDBB and DBBM were not significantly different. This phenomenon could be cause by increased anisotropy with increasing temperature and duration of heating. The pores are oriented longitudinally in thickness, microstructure anisotropy causes anisotropy of mechanical and functional properties (Cahyaningrum et al., 2018). During the deproteinization process, the pores are interconnected in 3D, the pores appear where they were occupied by protein matrix. Since the collagen fiber prefer to be

aligned in the direction of bone growth (longitudinal) the pores are oriented preferentially in this direction. According to the Fatihhi et al (2015) the degree of anisotropy bovine bone has average 0,599±0,139, so that three types of scaffolds in this study are still included in the criteria of a good scaffold.

Connectivity density is the number of trabeculae per unit volume, a high degree of interconnection is important to achieve good cell viability into the scaffold. The highest connectivity density was FDBB followed by DC- and the lowest was DBBM. Connectivity density value of FDBB, DC-FDBB, and DBBM were all higher than the value of bovine cancellous bone according to Fatihhi et al (2015) was 4,588±2,053 mm^{-3}. After the analysis, it was found DBBM and DC-FDBB had significantly different connectivity density, while DBBM and FDBB and DC-FDBB and FDBB were not significantly different. This can be caused by the heterogenous morphology and anisotropy of cancellous bovine bone, and there is no significant difference in the number of trabecular bone. The higher connectivity density value, the lower the porosity and thus increases the permeability of the scaffold. DC-FDBB with decellularization using SDS 0,5% for 24 hours damaged the trabeculae matrix, removes cytoplasm, damages cell membrane protein, remove 90% DNA content, glycosaminoglycan, collagen, and aggrecan, eliminate residual cell components such as osteoblast, osteocytes, hematopoietic elements in the extracellular matrix, and rinsing with PBS made the interconnection structure and the porosity and degree of anisotropy higher than FDBB while the DBBM had the highest porosity which made connectivity density of DBBM lower and made lower permeability (Morgan et al., 2004).

Bone surface density contributor to overall strength and fracture toughness, the structure scaffold, the trabeculae structure breaks in the lower bone surface density, weaker, thinner (Turunen et al., 2020). In this study, the bone surface density of FDBB scaffold were the highest at 5,936±0,370mm2/mm3 and the lowest were DBBM: 5,407±0,727mm2/mm3. From statistical calculations, there was no significant difference between the bone surface density of FDBB, DC-FDBB and DBBM, the value of three scaffolds is higher than value of bovine bone scaffold according to Fatihhi et al (2015) which is 0,201±0,022mm2/mm3. This is in accordance with theory that the pore surface area available for cellular attachment is inversely proportional to the pore size in it. DBBM standing alone is very fragile, so it is necessary to add collagen for better strength (Cahyaningrum et al., 2018).

The results showed that the largest structural model index size in the DC-FDBB was 0,573±0,093 and the smallest DBBM 0,185±0,068. The results in this study DC-FDBB have more rods trabecular geometry, while DBBM is more towards the plates. The change in structure from plate-like to rod-like indicates trabecular thinning (Benders et al., 2013). The SMI on DBBM and DC-FDBB and DBBM and FDBB were significantly different. Because heating up to 1000°C makes all organic components disappear, leaving only inorganic components, decomposition of carbonate minerals and transformation of hydroxyapatite into three calcium phosphate (β-TCP), this makes the porosity larger thus increases osteogenesis but decreases mechanical strength, large connectivity structure, conversely trabecular thickness being smaller, and Ca/P ratio is reduced thus resorption becomes slower and solubility decreases (Abdelmoneim et al., 2020; Niakan et al., 2015; Uklejewski et al., 2015). While decellularization using SDS 0,5% for 24 hours could destroy cytoplasm and cell membranes, eliminate cells and damages structure of extracellular matrix by removing glycosaminoglycans and water thus SMI DC-FDBB become larger to rod like (Benders et al., 2013; Gilpin & Yang, 2017; Ling et al., 2021; Malagón-Escandón et al., 2021).

The study limitations was there was no variability in the duration of immersion and in SDS concentration of decellularization agent, so further research is needed.

4. Conclusion

The comparison results of the microarchitecture of three different types of scaffolds for bone tissue engineering are as follows. According to the research, the DBBM (deproteinized bovine bone material) scaffold exhibits the most ideal 3D microarchitecture due to its highest porosity, largest pore size, highest degree of anisotropy, and smallest structural model index with trabecular plate geometry. On the other hand, the DC-FDBB (decellularized freeze-dried bovine bone) scaffold has the least ideal morphology, resembling a rod-like structure. These findings indicate the significant role of scaffold morphology in bone tissue engineering, with the DBBM scaffold possessing the most favorable properties for such applications. It was concluded that, the cancellous bovine scaffold with the most ideal microarchitecture 3D morphology were the DBBM scaffold because it have highest porosity, pore size, degree of anisotropy, and smallest structural model index with trabecular plate geometry and the least were DC-FDBB with rod like geometry.

Acknowledgements

Declaration of Interest
The authors of his manuscript declare no conflicts of interest in this article.

5. References

1. Abdelmoneim, D., Alhamdani, G. M., Paterson, T. E., Santocildes Romero, M. E., Monteiro, B. J. C., Hatton, P. V., & Asencio, I. O. (2020). Bioactive and topographically-modified electrospun membranes for the creation of new bone regeneration models. *Processes*, *8*(11). https://doi.org/10.3390/pr8111341
2. Ashworth, J. C., Best, S. M., & Cameron, R. E. (2014). Quantitative architectural description of tissue engineering scaffolds. In *Materials Technology* (Vol. 29, Issue 5). https://doi.org/10.1179/1753555714Y.0000000159
3. Bagwan, J. K., Ahuja, B. B., Mulay, A. V., & Jawale, K. J. (2021). Geometrical analysis of extrusion based (Additively Manufactured) 3D designed scaffold for bone tissue Engineering: A finite element approach. *Materials Today: Proceedings*, *50*. https://doi.org/10.1016/j.matpr.2021.09.049
4. Bahraminasab, M. (2020). Challenges on optimization of 3D-printed bone scaffolds. In *BioMedical Engineering Online* (Vol. 19, Issue 1). https://doi.org/10.1186/s12938-020-00810-2
5. Benders, K. E. M., Weeren, P. R. van, Badylak, S. F., Saris, D. B. F., Dhert, W. J. A., & Malda, J. (2013). Extracellular matrix scaffolds for cartilage and bone regeneration. In *Trends in Biotechnology* (Vol. 31, Issue 3). https://doi.org/10.1016/j.tibtech.2012.12.004
6. Bigham-Sadegh, A., & Oryan, A. (2015). Basic concepts regarding fracture healing and the current options and future directions in managing bone fractures. In *International Wound Journal* (Vol. 12, Issue 3). https://doi.org/10.1111/iwj.12231
7. Cahyaningrum, S. E., Herdyastuty, N., Devina, B., & Supangat, D. (2018). Synthesis and Characterization of Hydroxyapatite Powder by Wet Precipitation Method. *IOP Conference Series: Materials Science and Engineering*, *299*(1). https://doi.org/10.1088/1757-899X/299/1/012039
8. Cheung, H. Y., Lau, K. T., Lu, T. P., & Hui, D. (2007). A critical review on polymer-based bio-engineered materials for scaffold development. *Composites Part B: Engineering*, *38*(3). https://doi.org/10.1016/j.compositesb.2006.06.014

9. Cravedi, P., Farouk, S., Angeletti, A., Edgar, L., Tamburrini, R., Duisit, J., Perin, L., & Orlando, G. (2017). Regenerative immunology: the immunological reaction to biomaterials. In *Transplant International* (Vol. 30, Issue 12). https://doi.org/10.1111/tri.13068

10. Fatihhi, S. J., Harun, M. N., Abdul Kadir, M. R., Abdullah, J., Kamarul, T., Öchsner, A., & Syahrom, A. (2015). Uniaxial and Multiaxial Fatigue Life Prediction of the Trabecular Bone Based on Physiological Loading: A Comparative Study. *Annals of Biomedical Engineering*, *43*(10). https://doi.org/10.1007/s10439-015-1305-8

11. Ferdiansyah Mahyudin, N., & Utomo, D. N. (2018). *Graft Tulang & Material Pengganti Tulang (Karaktersitik Dan Strategi Aplikasi Klinis)*. Airlangga University Press.

12. Galia, C. R., Lourenço, A. L., Rosito, R., Souza Macedo, C. A., & Camargo, L. M. A. Q. (2011). PHYSICOCHEMICAL CHARACTERIZATION OF LYOPHILIZED BOVINE BONE GRAFTS. *Revista Brasileira de Ortopedia (English Edition)*, *46*(4). https://doi.org/10.1016/s2255-4971(15)30260-3

13. Gardin, C., Ricci, S., Ferroni, L., Guazzo, R., Sbricoli, L., De Benedictis, G., Finotti, L., Isola, M., Bressan, E., & Zavan, B. (2015). Decellularization and delipidation protocols of bovine bone and pericardium for bone grafting and guided bone regeneration procedures. *PLoS ONE*, *10*(7). https://doi.org/10.1371/journal.pone.0132344

14. Gilpin, A., & Yang, Y. (2017). Decellularization Strategies for Regenerative Medicine: From Processing Techniques to Applications. In *BioMed Research International* (Vol. 2017). https://doi.org/10.1155/2017/9831534

15. Humidat, A. K. M., Kamadjaja, D. B., Bianto, C., Rasyida, A. Z., & Harijadi, A. (2018). Effect of freeze-dried bovine bone xenograft on tumor necrosis factor-alpha secretion in human peripheral blood mononuclear cells. *Asian Jr. of Microbiol. Biotech. Env. Sc*, *20*, S88–S92.

16. Kamadjaja, D. B., Harijadi, A., Soesilawati, P., Wahyuni, E., Maulidah, N., Fauzi, A., Rah Ayu, F., Simanjuntak, R., Soesanto, R., Asmara, D., Rizqiawan, A., Agus, P., & Pramono, C. (2017). Demineralized Freeze-Dried Bovine Cortical Bone: Its Potential for Guided Bone Regeneration Membrane. *International Journal of Dentistry*, *2017*. https://doi.org/10.1155/2017/5149675

17. Kartikasari, N., Yuliati, A., & Kriswandini, I. L. (2016). Compressive strength and porosity tests on bovine hydroxyapatite-gelatin-chitosan scaffolds. *Dental Journal (Majalah Kedokteran Gigi)*, *49*(3). https://doi.org/10.20473/j.djmkg.v49.i3.p153-157

18. Krieghoff, J., Picke, A. K., Salbach-Hirsch, J., Rother, S., Heinemann, C., Bernhardt, R., Kascholke, C., Möller, S., Rauner, M., Schnabelrauch, M., Hintze, V., Scharnweber, D., Schulz-Siegmund, M., Hacker, M. C., Hofbauer, L. C., & Hofbauer, C. (2019). Increased pore size of scaffolds improves coating efficiency with sulfated hyaluronan and mineralization capacity of osteoblasts. *Biomaterials Research*, *23*(1). https://doi.org/10.1186/s40824-019-0172-z

19. Lawrence, B. J., & Madihally, S. V. (2008). Cell colonization in degradable 3D porous matrices. In *Cell adhesion & migration* (Vol. 2, Issue 1). https://doi.org/10.4161/cam.2.1.5884

20. Lei, P., Sun, R., Wang, L., Zhou, J., Wan, L., Zhou, T., & Hu, Y. (2015). A new method for xenogeneic bone graft deproteinization: Comparative study of radius defects in a rabbit model. *PLoS ONE*, *10*(12). https://doi.org/10.1371/journal.pone.0146005

21. Li, J., You, F., Li, Y., Zuo, Y., Li, L., Jiang, J., Qu, Y., Lu, M., Man, Y., & Zou, Q. (2016). Bone regeneration and infiltration of an anisotropic composite scaffold: an experimental study of rabbit cranial defect repair. *Journal of Biomaterials Science,*

Polymer Edition, *27*(4), 327–338.

22. Liang, H., Chao, L., Xie, D., Yang, Y., Shi, J., Zhang, Y., Xue, B., Shen, L., Tian, Z., & Li, L. (2022). Trabecular-like Ti–6Al–4V scaffold for bone repair: A diversified mechanical stimulation environment for bone regeneration. *Composites Part B: Engineering*, *241*, 110057.

23. Ling, Y., Xu, W., Yang, L., Liang, C., & Xu, B. (2021). Improved the biocompatibility of cancellous bone with compound physicochemical decellularization process. *Regenerative Biomaterials*, *7*(5). https://doi.org/10.1093/RB/RBAA024

24. Malagón-Escandón, A., Hautefeuille, M., Jimenez-Díaz, E., Arenas-Alatorre, J., Saniger, J. M., Badillo-Ramírez, I., Vazquez, N., Piñón-Zarate, G., & Castell-Rodríguez, A. (2021). Three-dimensional porous scaffolds derived from bovine cancellous bone matrix promote osteoinduction, osteoconduction, and osteogenesis. *Polymers*, *13*(24). https://doi.org/10.3390/polym13244390

25. Matsukawa, S., Makino, T., Mori, S., Koyama, D., Takayanagi, S., Mizuno, K., Yanagitani, T., & Matsukawa, M. (2017). Effect of anisotropy on stress-induced electrical potentials in bovine bone using ultrasound irradiation. *Applied Physics Letters*, *110*(14).

26. Migliaresi, C., & Motta, A. (2014). Scaffolds for tissue engineering: Biological design, materials, and fabrication. In *Scaffolds for Tissue Engineering: Biological Design, Materials, and Fabrication*. https://doi.org/10.4032/9789814463218

27. Mitchell, G. R., & Tojeira, A. (2013). 3rd international conference on tissue engineering, ICTE2013 role of anisotropy in tissue engineering. *Procedia Engineering*, *59*. https://doi.org/10.1016/j.proeng.2013.05.100

28. Morgan, E. F., Bayraktar, H. H., Yeh, O. C., Majumdar, S., Burghardt, A., & Keaveny, T. M. (2004). Contribution of inter-site variations in architecture to trabecular bone apparent yield strains. *Journal of Biomechanics*, *37*(9). https://doi.org/10.1016/j.jbiomech.2003.12.037

29. Murphy, C. M., O'Brien, F. J., Little, D. G., & Schindeler, A. (2013). Cell-scaffold interactions in the bone tissue engineering triad. In *European Cells and Materials* (Vol. 26). https://doi.org/10.22203/eCM.v026a09

30. Nelms, L., & Palmer, W. J. (2019). Tissue engineering in mandibular reconstruction: osteogenesis-inducing scaffolds. In *Plastic and Aesthetic Research* (Vol. 6). https://doi.org/10.20517/2347-9264.2019.40

31. Niakan, A., Ramesh, S., Tan, C. Y., Purbolaksono, J., Chandran, H., & Teng, W. D. (2015). Effect of annealing treatment on the characteristics of bovine bone. *Journal of Ceramic Processing Research*, *16*(2).

32. Oftadeh, R., Perez-Viloria, M., Villa-Camacho, J. C., Vaziri, A., & Nazarian, A. (2015). Biomechanics and Mechanobiology of Trabecular Bone: A Review. In *Journal of Biomechanical Engineering* (Vol. 137, Issue 1). https://doi.org/10.1115/1.4029176

33. Oryan, A., Alidadi, S., Moshiri, A., & Maffulli, N. (2014). Bone regenerative medicine: Classic options, novel strategies, and future directions. In *Journal of Orthopaedic Surgery and Research* (Vol. 9, Issue 1). https://doi.org/10.1186/1749-799X-9-18

34. Sandberg, O. H., & Aspenberg, P. (2016). Inter-trabecular bone formation: a specific mechanism for healing of cancellous bone: A narrative review. *Acta Orthopaedica*, *87*(5), 459–465.

35. Sari, M., Kristianto, N. A., Chotimah, Ana, I. D., & Yusuf, Y. (2021). Carbonated hydroxyapatite-based honeycomb scaffold coatings on a titanium alloy for bone implant application—physicochemical and mechanical properties analysis. *Coatings*, *11*(8). https://doi.org/10.3390/coatings11080941

36. Shahabipour, F., Mahdavi-Shahri, N., Matin, M. M., Tavassoli, A., & Zebarjad, S. M.

(2013). Scaffolds derived from cancellous bovine bone support mesenchymal stem cells' maintenance and growth. *In Vitro Cellular and Developmental Biology - Animal*, *49*(6). https://doi.org/10.1007/s11626-013-9591-7

37. Soleimanifar, M., & Katoozian, H. R. (2013). *Energy Based Simulation of Trabecular Bone Fracture Healing Using Finite Element and Fuzzy Logic*.

38. Stiehl, J. B. (2005). Trabecular metal in hip reconstructive surgery. *Orthopedics*, *28*(7), 662–670.

39. Stuckensen, K., Lamo-Espinosa, J. M., Muiños-López, E., Ripalda-Cemboráin, P., López-Martínez, T., Iglesias, E., Abizanda, G., Andreu, I., Flandes-Iparraguirre, M., & Pons-Villanueva, J. (2019). Anisotropic cryostructured collagen scaffolds for efficient delivery of RhBMP–2 and enhanced bone regeneration. *Materials*, *12*(19), 3105.

40. Turunen, M. J., Le Cann, S., Tudisco, E., Lovric, G., Patera, A., Hall, S. A., & Isaksson, H. (2020). Sub-trabecular strain evolution in human trabecular bone. *Scientific Reports*, *10*(1). https://doi.org/10.1038/s41598-020-69850-x

41. Uklejewski, R., Winiecki, M., Musielak, G., & Tokłowicz, R. (2015). Effectiveness of various deproteinization processes of bovine cancellous bone evaluated via mechano-biostructural properties of produced osteoconductive biomaterials. *Biotechnology and Bioprocess Engineering*, *20*(2). https://doi.org/10.1007/s12257-013-0510-2